Organic & Biomolecular Chemistry

Cite this: *Org. Biomol. Chem.*, 2011, **9**, 463

www.rsc.org/obc

PAPER

Tetracycline prevents Aβ oligomer toxicity through an atypical supramolecular interaction†

Cristina Airoldi,[a] Laura Colombo,[b] Claudia Manzoni,[b] Erika Sironi,[a] Antonino Natalello,[a] Silvia Maria Doglia,[a] Gianluigi Forloni,[b] Fabrizio Tagliavini,[c] Elena Del Favero,[d] Laura Cantù,[d] Francesco Nicotra*[a] and Mario Salmona[b]

Received 22nd June 2010, Accepted 20th September 2010
DOI: 10.1039/c0ob00303d

The antibiotic tetracycline was reported to possess an anti-amyloidogenic activity on a variety of amyloidogenic proteins both in *in vitro* and *in vivo* models. To unveil the mechanism of action of tetracycline on Aβ1–40 and Aβ1–42 at both molecular and supramolecular levels, we carried out a series of experiments using NMR spectroscopy, FTIR spectroscopy, dynamic laser light-scattering (DLS) and atomic force microscopy (AFM). Firstly we showed that the co-incubation of Aβ1–42 oligomers with tetracycline hinders the toxicity towards N2a cell lines in a dose-dependent manner. Therefore, the nature of the interaction between the drug and Aβ oligomers was investigated. To carry out NMR and FTIR studies we have prepared Aβ peptide solutions containing assemblies ranging from monomers to large oligomers. Saturation transfer difference (STD) NMR experiments have shown that tetracycline did not interact with monomers at variance with oligomers. Noteworthy, in this latter case we observed that this interaction was very peculiar since the transfer of magnetization from Aβ oligomers to tetracycline involved all drug protons. In addition, intermolecular cross-peaks between tetracycline and Aβ were not observed in NOESY spectra, indicating the absence of a specific binding site and suggesting the occurrence of a supramolecular interaction. DLS and AFM studies supported this hypothesis since the co-dissolution of Aβ peptides and tetracycline triggered the immediate formation of new aggregates that improved the solubility of Aβ peptides, preventing in this way the progression of the amyloid cascade. Moreover, competitive NMR binding experiments showed for the first time that tetracycline competes with thioflavin T (ThT) in the binding to Aβ peptides. Our data shed light on a novel mechanism of anti-amyloidogenic activity displayed by tetracycline, governed by hydrophobic and charge multiparticle interactions.

Introduction

Alzheimer's disease (AD) is a neurodegenerative disorder that affects over 30 million individuals worldwide. Despite extensive research there is still no effective treatment; pharmacological intervention is limited to symptomatic therapy with cholinergic drugs and glutamatergic partial antagonists. As a result, AD has a severe impact on patients and their families' quality of life, and its economic burden is massive. A central pathological feature of AD is the accumulation of misfolded amyloid β (Aβ) peptides in the form of oligomers and amyloid fibrils in the brain.[1–4]

Aggregated Aβ species, particularly oligomeric assembly intermediates, are believed to trigger a cascade of events that lead to protein tau hyperphosphorylation, misfolding and assembly into abnormal filaments with the formation of neurofibrillary tangles and disruption of the neuronal cytoskeleton, widespread synaptic loss and neurodegeneration.[5] A substantial effort has been made in the last 20 years to develop AD therapies. The considerable efforts in the design of Aβ targeting molecules have been useful, providing several classes of compounds with different modes of activity, but the drugs selected for clinical trials have given unsatisfactory results or caused adverse events, and there is still an urgent need for safe and effective molecules for AD treatment.

[a]*Department of Biotechnology and Biosciences, University of Milano-Bicocca, Pzza della Scienza 2, 20126, Milan, Italy. E-mail: francesco.nicotra@unimib.it; Fax: +390264483565; Tel: +390264482152*

[b]*Department of Molecular Biochemistry and Pharmacology and Department of Neuroscience Mario Negri Institute for Pharmacological Research, Via La Masa 19, 20156, Milan, Italy*

[c]*Division of Neurology and Neuropathology, "Carlo Besta" National Neurological Institute, Via Celoria 11, 20133, Milan, Italy*

[d]*Department of Chemistry, Biochemistry and Biotechnologies for Medicine, University of Milano, LITA, V. F.lli Cervi, 93, 20090, Segrate, (MI), Italy*

† Electronic supplementary information (ESI) available: S1 – NMR Characterization of Aβ1-40 and Aβ1-42 assembly; S2 – Aβ1-40 and Aβ1-42 STD-NMR; S3 – Diffusion data deconvolution; S4 – Aβ1-42 trNOESY; S5 – Aβ1-40 and Aβ1-42 titration with tetracycline; S6 – CD spectra of Aβ1-42 in the presence of tetracycline; S7 – Atomic Force Microscopy. Analysis of aggregate height formed following co-dissolution of Aβ peptides with tetracycline; S8 – Tetracycline–Thioflavin T competitive binding studies; S9 – FTIR spectra of Aβ peptides in presence of thioflavin T. See DOI: 10.1039/c0ob00303d

Based on structural analogies with Congo red, tetrapyrroles and acridine derivatives, we hypothesized that tetracyclines might interact with the disease-related isoform of prion protein (PrPSc) and misfolded Aβ peptides. We have shown that tetracyclines promote PrPSc and Aβ degradation by proteases, inhibit the aggregation of amyloidogenic peptides PrP106–126 and PrP82–146 and of Aβ and destabilize aggregates. The anti-amyloidogenic effect of tetracyclines has also been confirmed with other amyloidogenic proteins, such as transthyretin, W7FW14F apomyoglobin, amylin, huntingtin, α2-macroglobulin, α-synuclein, poly(A) binding protein nuclear 1[6] in *in vitro* and *in vivo* models.

Tetracyclines include several congeners. They have relatively low toxicity and some of them, such as doxycycline and minocycline, efficiently cross the blood brain barrier. Tetracyclines have an amphiphilic character, due to their extended hydrophobic core formed of aromatic moieties, with a large number of hydrophilic substituents. Derived from a common hydronaphthacene nucleus containing four fused rings, these compounds have various substitutions at positions 5, 6 and 7 and five asymmetric centers: C-4, C-4a, C-5a, C-6 and C-12a. Scheme 1 reports the structure of tetracycline.

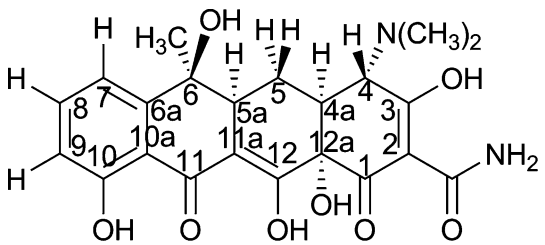

Scheme 1 Tetracycline structure; numbering of hydrogens and carbons.

Multiple functional groups with acidic-base properties contribute to their high solubility in polar organic solvents and water, which is enhanced at low pH. Most of them have an isoelectric point between 4 and 6 due to their amphoteric character. In the hydrochloride form, tetracyclines had four potentially dissociable proton centers, namely C1-C3 tricarbonyl methane, O-10 and O-12 ketophenolic hydroxyl groups and C-4 dimethylammonium group. However, the formation of intra- and inter-molecular hydrogen bonds and the conformational change due to the dielectric constant of the medium interfere in the deprotonation scheme. Tetracyclines undergo complex formation with a variety of metal cations (such as Ca^{2+}, Mg^{2+}, Cu^{2+}, Co^{2+} and Ni^{2+}) and they are transported in plasma as a calcium complex.

Based on the *in vitro* and preclinical *in vivo* data, a randomized double-blind phase II study for the evaluation of the efficacy of doxycycline in patients with Creutzfeldt-Jakob disease has been approved and funded by the Italian Agency for Drugs (*Europian Clinical Trials Database*; *Identifier*: *2006-001858-27*). Moreover, a phase II clinical trial is also ongoing in patients suffering from transthyretin amyloidosis (*ClinicalTrials.gov*; *Identifier*: *NCT01171859*). These observations prompted us to focus more in detail on Aβ and study whether these drugs antagonize the cytotoxic effects of the oligomeric forms of Aβ, and explore in detail their anti-fibrillogenic mode of action at the molecular level. In this paper we show that tetracycline, when co-dissolved with Aβ, forms immediately supramolecular complexes, preventing the formation of fibrillar aggregates and the progression of the amyloid cascade. We hypothesize that this mechanism of action may be extended to other amyloidogenic proteins as well.

Results and discussion

In vitro toxicity assay

The toxicity of Aβ1–42 on N2a cells was studied in the concentration range of 5–500 nM. Pre-incubation of Aβ1–42 with tetracycline for 70 h at molar ratios of 1 : 4 or 1 : 8 significantly reduced peptide toxicity after 24 h of exposure (Fig. 1a). Western Blot and Dot Blot analysis confirmed the presence of oligomers in the fresh peptide solution (Fig. 1b and c).

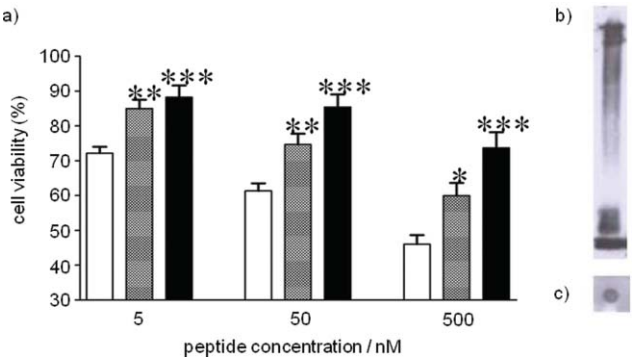

Fig. 1 *In vitro* Aβ toxicity assay. a) Viability of N2a cells after 24 h of exposure to 5–500 nM Aβ1–42. White bars, Aβ1–42 alone; grey bars, Aβ1–42 - tetracycline at a 1 : 4 molar ratio; black bars, Aβ1–42 - tetracycline at a 1 : 8 molar ratio. Error bars are the SEM of 4 replicates. *** $p < 0.0001$; ** $p < 0.001$; * $p < 0.01$ *vs.* Aβ1–42 alone by one way ANOVA followed by the Dunnett post-hoc test. b) Western Blot and c) Dot Blot analysis of freshly dissolved Aβ1–42 performed using 6E10 and A11 antibodies, respectively.

To elucidate the mechanism of action of tetracycline protection against neurotoxicity we investigated its interaction with Aβ1–40 and Aβ1–42 by NMR spectroscopy, AFM, FTIR and DLS.

NMR and FTIR characterization of Aβ peptides in solution

^{1}H-NMR line width broadening monitoring and PFG-NMR diffusion measurements[7,8] were carried out at 5, 25 or 37 °C with both peptides in the concentration range of 50–500 μM. The analysis of the experiments showed that they were mostly in oligomeric forms in PBS, pH 7.4. Conversely, when Aβ1–40 was dissolved in PBS, pH 12, at 5 °C, or in DMSO[9] at 37 °C, it acquired an unordered monomeric structure, as deduced from ^{1}H-NMR line width narrowing (compared to spectra at pH 7.4) and FTIR analysis, as described below (Fig. 3). ^{1}H-NMR spectra acquired on the same Aβ1–40 or Aβ1–42 samples dissolved in PBS at pH 7.4 or pH 12, 5 °C are reported in Fig. 2.

For both peptides, S/N ratios were higher and ^{1}H-NMR signals sharper in the spectrum recorded at pH 12, also in agreement with the measurements of relaxation times, which showed higher T1 and selective T1 values under these experimental conditions (ESI†, S1 – Tables 1S and 2S).

NMR diffusion measurements allowed a further characterization of Aβ peptide oligomers at pH 7.4. Calibration curves correlating molecular weights with diffusion coefficients (logD *vs.*

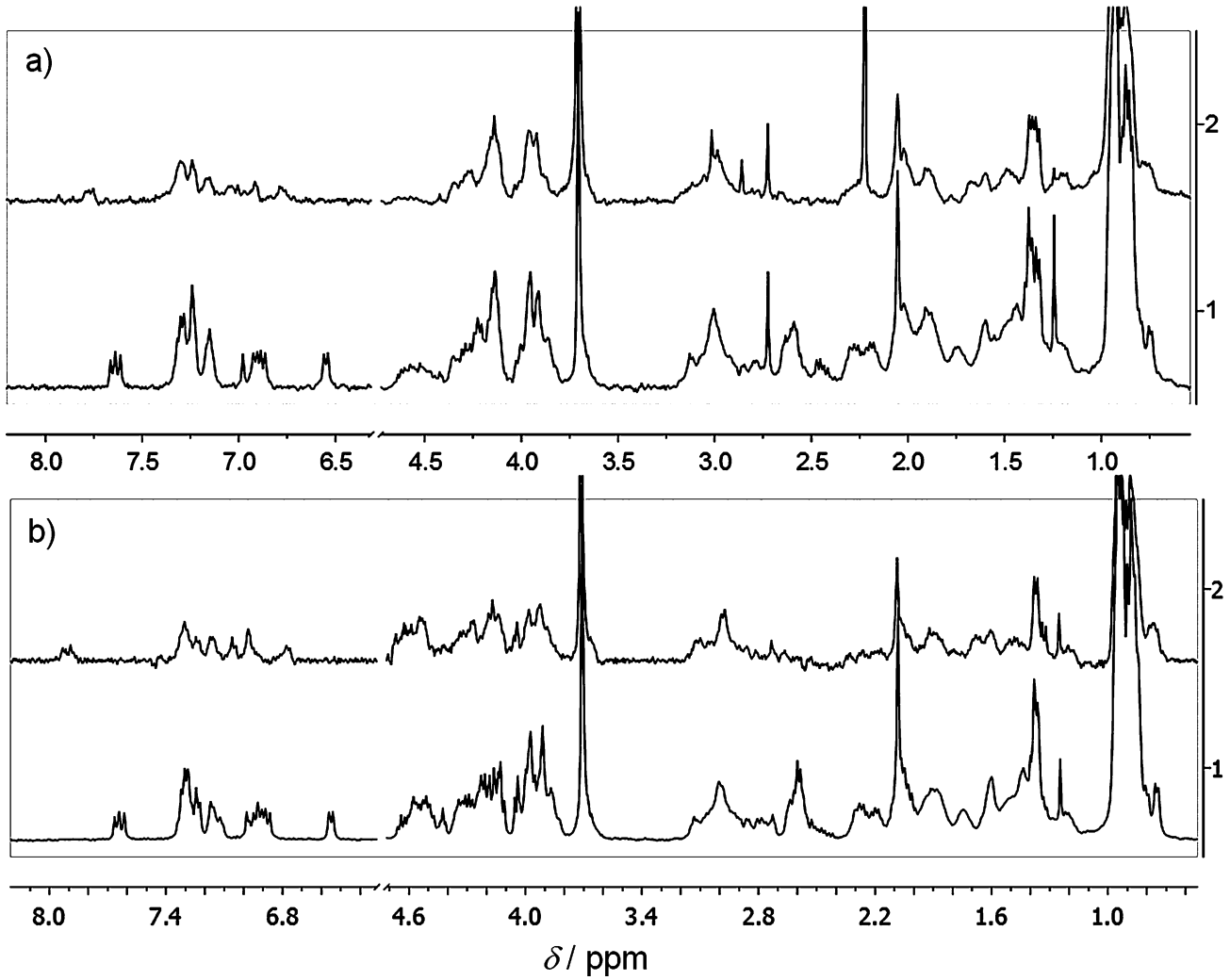

Fig. 2 a) ^{1}H-NMR spectra of 0.5 mM Aβ1–40 acquired in PBS, pH 12 (1) or at pH 7.4 (2, enhanced 2×), 5 °C, number of scans (NS) = 128. b) ^{1}H-NMR spectra of 0.25 mM Aβ1–42 acquired in PBS, pH 12 (1) or at pH 7.4 (2, enhanced 6×), 5 °C, NS = 512.

Table 1 Aβ1–40 diffusion coefficients in solution at 5, 25 or 37 °C, pH 7.4

pH	*T*/°C	Expected diff. coeff. for the monomer	Observed diffusion coefficient[a]	Δ
7.4	5	0.845 10^{-10} m^2 s^{-1}	0.745 10^{-10} m^2 s^{-1}	– 11.8%
7.4	25	1.626 10^{-10} m^2 s^{-1}	1.378 10^{-10} m^2 s^{-1}	– 15.2%
7.4	37	2.841 10^{-10} m^2 s^{-1}	1.862 10^{-10} m^2 s^{-1}	– 34.5%

[a] uncertainty less than 1%.

logMW) were used to estimate *D* values for Aβ peptide monomers and small oligomers at 5, 25 or 37 °C.[10] Protein size standards employed were bradykinin (1090 Da), bovine insulin (5734 Da, not used for the calibration curve at 37 °C),[11] ubiquitin (8500 Da), cytochrome C (13 000 Da), lysozyme (14 700 Da). Expected and observed D values for Aβ1–40 at different temperatures (5, 25 or 37 °C) at pH 7.4 are reported in Table 1; DOSY spectra are depicted in ESI†, S1 – Figure 1S.

The measured coefficients at 5 and 25 °C, pH 7.4 were consistent with the presence of a mixture of monomers and small oligomers, with *D* values being lower than expected for the monomer (–11.8% and –15.2% respectively). The diffusion coefficient at 37 °C was 65.5% of that estimated for the monomer, as expected as a consequence of the temperature-dependence of Aβ peptide aggregation. In particular, due to the short T2 values of large aggregates, it is realistic to assume that they do not significantly contribute to the high-resolution NMR spectrum (it is indeed a NMR-silent species) and that the major contributions to the observed decrease of the resonance intensity in the diffusion experiment depends on the formed monomeric, dimeric and trimeric peptides. In the case of Aβ1–42, due to the low intensity of ^{1}H peptide signals, an uncertainty greater than 6.0% was obtained for experiments carried out at pH 7.4, even when the spectra were acquired with a high number of scans (512) (Fig. 2b). Longer acquisition times were not possible due to peptide aggregation and precipitation. For this reason, data on Aβ1–42 were considered unreliable and are not reported here.

FTIR spectroscopy indicated that both Aβ peptides formed oligomers with major β-sheet intermolecular interactions in PBS, pH 7.4 (Fig. 3). The FTIR spectrum of Aβ peptides in D_2O PBS buffer, pH 7.4, displayed two bands at ~1,622 and ~1,686 cm^{-1} for Aβ1–40 and at ~1,625 and ~1,686 cm^{-1} for Aβ1–42. These bands

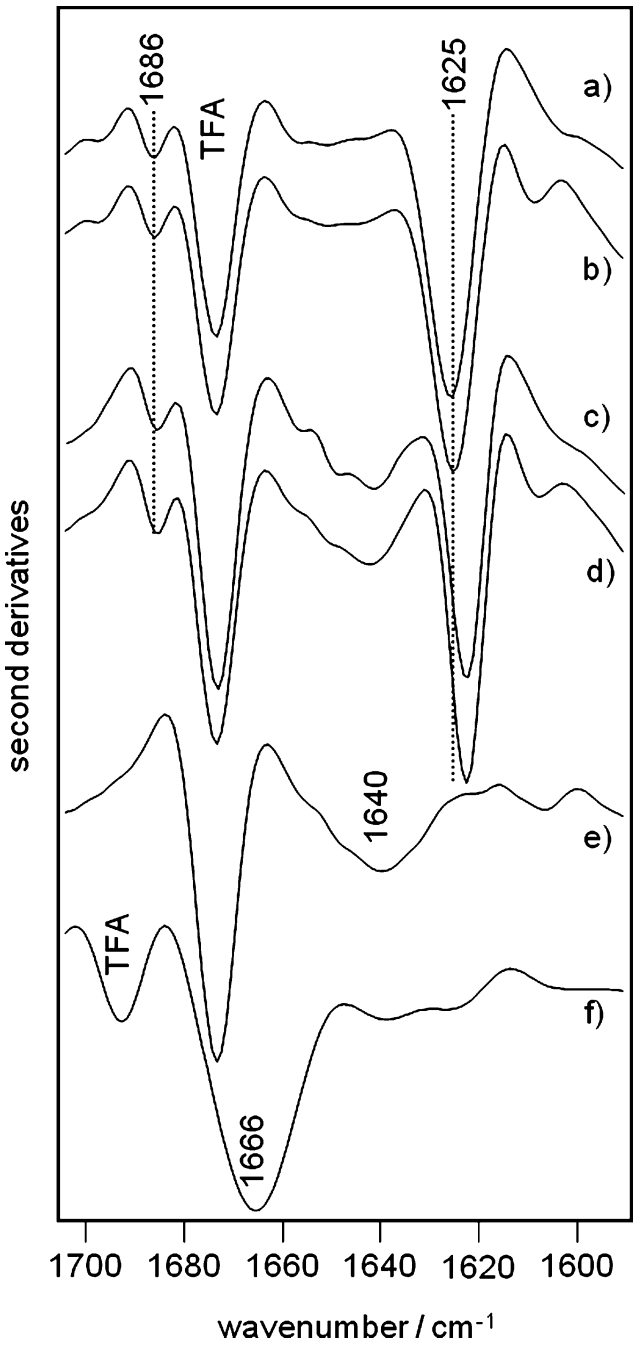

Fig. 3 Second derivative FTIR absorption spectra of Aβ1–42 and Aβ1–40 in presence or absence of tetracycline. Spectra of Aβ1–42 in D_2O PBS buffer, pH 7.4 in absence (a) and in presence (b) of tetracycline at a 1 : 4 molar ratio. Spectra of Aβ1–40 in D_2O PBS, pH 7.4 in absence (c) and in presence (d) of tetracycline at a 1 : 2 molar ratio. Spectra of Aβ1–40 in D_2O PBS, pH 12 (e) and in deuterated DMSO (f), both in presence of tetracycline at a 1 : 2 molar ratio. The 1,673 cm^{-1} peak in D_2O buffers (a–e) and the 1,692 cm^{-1} peak in DMSO (f) are respectively due to the infrared response of residual TFA.

are the specific signature of intermolecular β-sheet interactions in oligomers,[12,13] but they could be also due to β-hairpin structures.[14] Recently, it has been demonstrated that the infrared response of Aβ1–42[13] and of Aβ1–40[12] oligomers in the Amide I region consists of two intermolecular β-sheet bands, whereas fibrils lead only to the lowest wavenumber band,[13] as already observed for a prion peptide.[15] The FTIR spectrum of both peptides showed an additional broad band around 1,642 cm^{-1} (more intense in the case of Aβ1–40) that can be assigned to the peptide unordered structure.[16]

This last result may suggest that Aβ1–40 oligomers are present at lower extent compared with Aβ1–42, in agreement with its higher aggregation propensity. On the contrary, the spectra of Aβ1–40 in PBS, pH 12 and in deuterated DMSO (data not shown) displayed, respectively, only an absorption band at ~1,640 cm^{-1} and ~1,666 cm^{-1} that can be assigned to the peptide unordered structure in D_2O[16] and in DMSO.[17] We can therefore conclude that, under these conditions, the peptide is in a monomeric form and does not aggregate into oligomers with intermolecular β-sheet structures.

Thus, NMR and FTIR findings consistently demonstrated that the Aβ peptides form oligomers at pH 7.4; this result is further supported by the AFM data reported below. In addition, these data support a higher level of oligomerization for Aβ1–42 *vs.* Aβ1–40. On the other hand, when dissolved in PBS, pH 12, or in DMSO, Aβ1–40 was found to be in unordered monomeric form. In light of these results, we decided to use these different experimental conditions to generate samples representative of the different aggregation states of Aβ peptides.

Binding of tetracycline to Aβ oligomers

Different NMR experimental approaches were used to evaluate the interaction of Aβ peptides with tetracycline. Saturation transfer difference (STD) NMR experiments[18–21] in PBS, pH 7.4, provided clear evidence of tetracycline binding to the Aβ1–40 and Aβ1–42 oligomers. STD spectra at peptide : tetracycline molar ratios from 1 : 2 to 1 : 30 were acquired employing different saturation times and temperatures (Fig. 4 and ESI†, S2). In all cases, after selective irradiation of the peptide resonances, tetracycline signals appeared in the STD spectra indicating the existence of magnetization transfer from the oligomers to the drug. A detailed ligand-epitope mapping was not possible because each tetracycline proton showed the corresponding STD signal.

Additional evidence for tetracycline binding to Aβ oligomers was obtained by measuring its diffusion coefficient at different peptide : drug molar ratios by PFG-NMR. Calibration curves correlating molecular weight with diffusion coefficient (logD *vs.* logMW) were used to estimate *D* values for tetracycline monomers at 5, 25 or 37 °C.[10] Molecular size standards employed were glucose (180 Da), lactose (342 Da), raffinose (504 Da), bradykinin (1040 Da). Expected and observed *D* values for tetracycline in absence or in presence of Aβ peptides at 5 °C, pH 7.4 or pH 12, are reported in Table 2. Tetracycline diffusion coefficients decreased significantly at increasing peptide : drug molar ratios, as expected for its interaction with a large molecular weight species.[22,23] Conversely, when Aβ1–40 was dissolved in PBS, pH 12, at 5 °C, or in DMSO at 37 °C, acquiring an unordered monomeric structure, the tetracycline diffusion coefficient measured on tetracycline-peptide mixtures was unchanged, indicating the absence of drug-peptide interactions (Table 2),[24] and STD spectra showed only Aβ1–40 signals (ESI†, S2).

To detect Nuclear Overhauser Effect (NOE) contacts between tetracycline protons and peptide residues, 2D-NOESY spectra

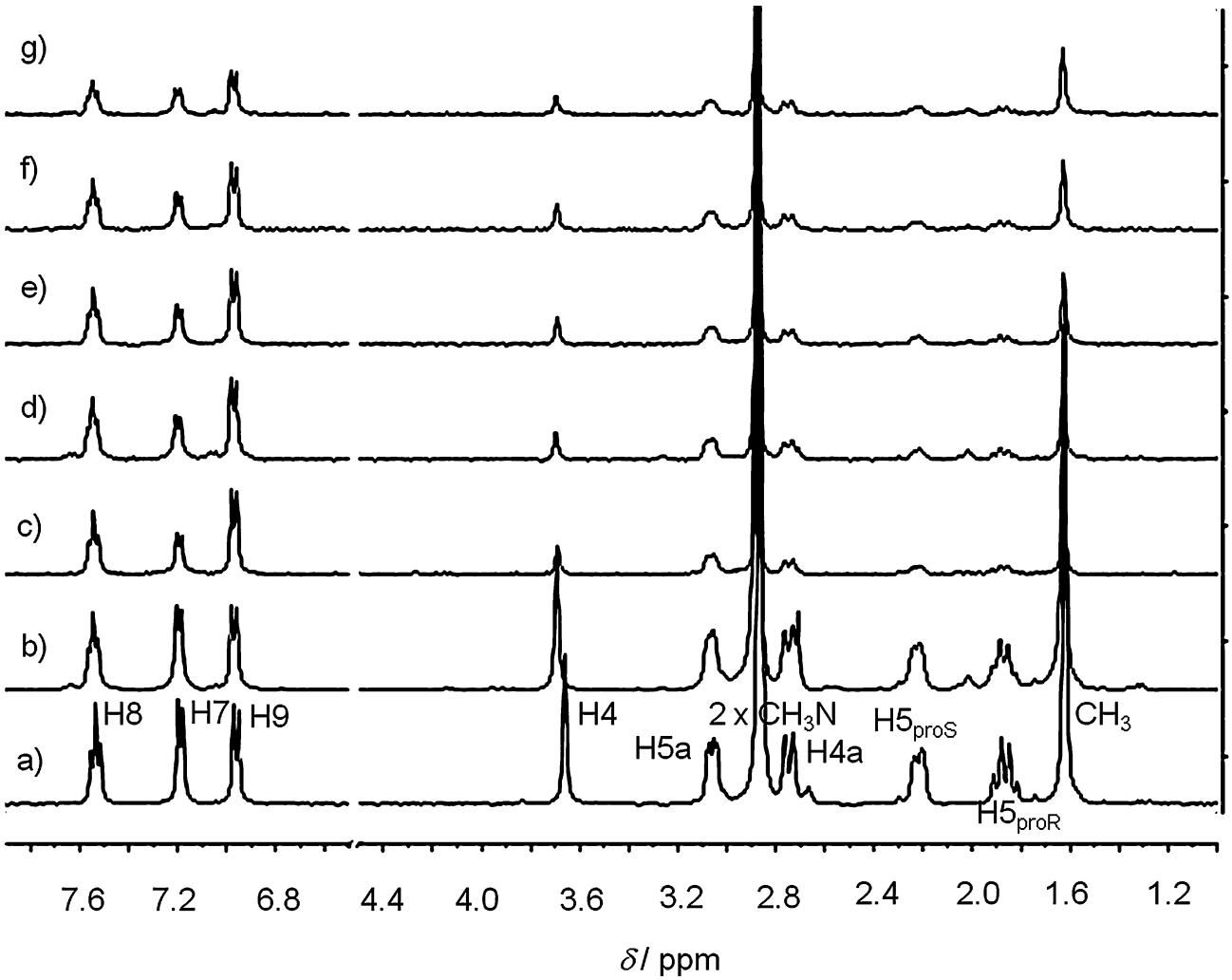

Fig. 4 a) ^{1}H-NMR spectra of tetracycline, NS = 32. b) Aβ1–42-tetracycline mixture, at a 1 : 30 molar ratio, NS = 32. c–g), STD spectra of the mixture recorded at different peptide saturation times (c, 5 s; d, 3 s; e, 2 s; f, 1.2 s; g, 0.5 s). NS = 896, on-resonance frequency = –1.0 ppm, off-resonance frequency = 40 ppm. Spectra b–g were recorded on the same sample; all samples were dissolved in PBS, pH 7.4, at 25 °C.

Table 2 Tetracycline diffusion coefficients in absence or presence of Aβ peptides at 5 °C, pH 7.4 or pH 12

Aβ sequence	pH	Peptide : tetracycline ratio	Diffusion coefficient[a]
—	7.4	tetracycline alone	2.059 10^{-10} m^2 s^{-1}
1–40	7.4	1 : 2	1.620 10^{-10} m^2 s^{-1}
1–42	7.4	1 : 2	1.589 10^{-10} m^2 s^{-1}
1–42	7.4	1 : 4	1.691 10^{-10} m^2 s^{-1}
1–42	7.4	1 : 8	1.762 10^{-10} m^2 s^{-1}
—	12	tetracycline alone	2.021 10^{-10} m^2 s^{-1}
1–40	12	1 : 2	1.959 10^{-10} m^2 s^{-1}

[a] uncertainty less than 1%.

of the peptide-drug mixtures were acquired with mixing times ranging from 0.1 s to 0.65 s. These experiments permitted to confirm the existence of tetracycline intermolecular interactions with both Aβ1–40 and Aβ1–42 as deduced by the observed drug cross-peak change of sign (trNOE) (Fig. 5a, b; ESI†, S4). For isolated tetracycline, the NOE cross peaks were positive, *i.e.* their signs were opposite with respect to the diagonal peaks as expected for a small molecule with a short correlation time. However, a change of sign occurred in the presence of Aβ1–40 or Aβ1–42 indicating an increase in the correlation time, supporting the existence of interaction with the peptides.[18,25] Nevertheless, the fine details of the interaction at atomic resolution could not be deduced, since no intermolecular cross-peaks between tetracycline and Aβ peptides were identified, and no significant changes in the peptide chemical shifts were observed after titration with the drug (ESI†, S5). On the other hand, tetracycline cross-peaks maintained their positive signs in NOESY spectra recorded at pH 12 or in DMSO in the presence of Aβ1–40 (Fig. 5c–f), confirming the absence of binding to Aβ1–40 monomers under these experimental conditions. As Aβ monomers are the species mostly represented in Aβ1–40 and Aβ1–42 ^{1}H-NMR spectra, the absence of changes in the peptide chemical shifts and of intermolecular cross-peaks between tetracycline and Aβ peptides could also be due to the lack of interaction between tetracycline and Aβ monomers.

We also verified the influence of tetracycline on the structural properties of Aβ peptides by FTIR and circular dichroism (CD;

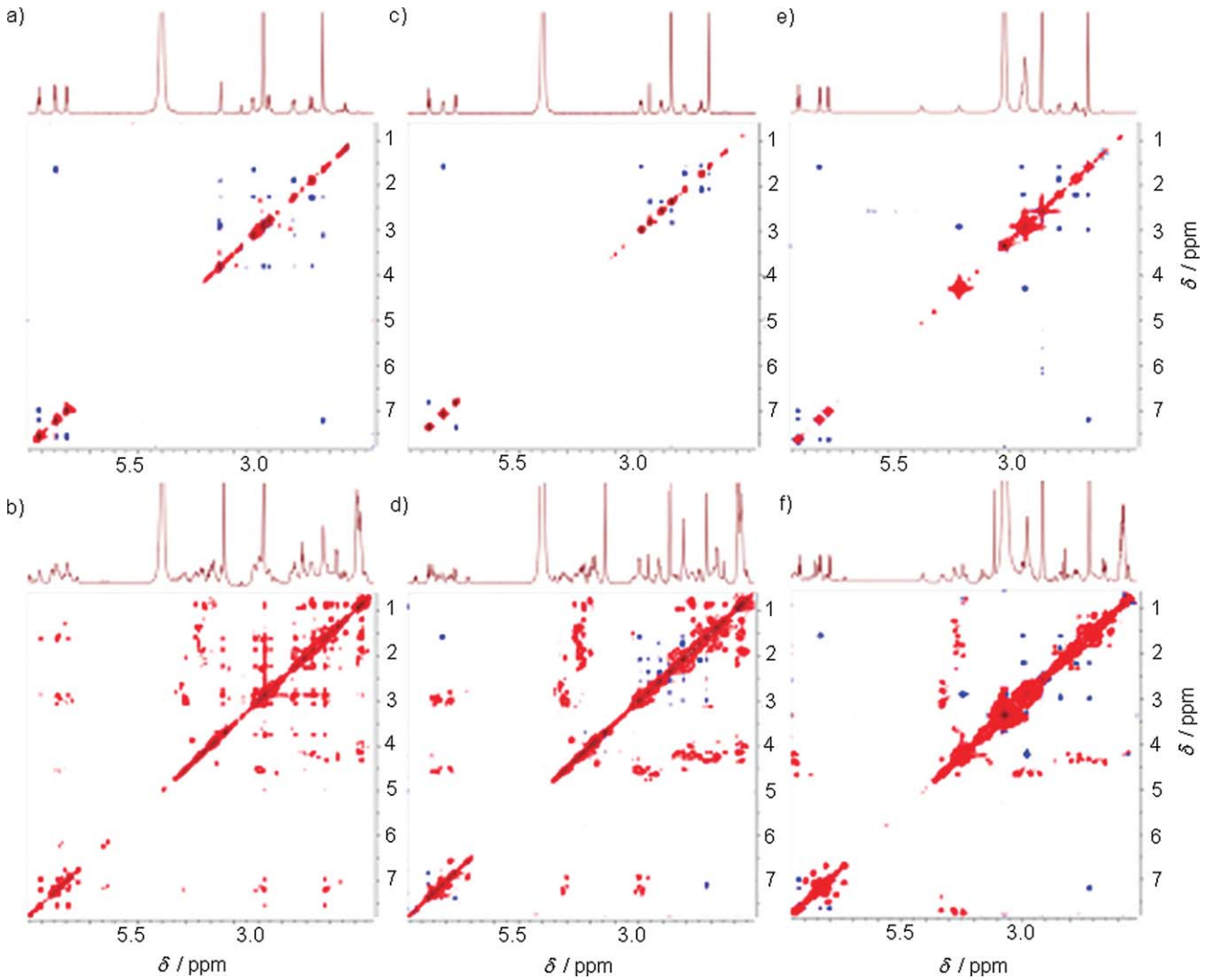

Fig. 5 2D-NOESY spectra of tetracycline in the absence (a, mix 650 ms, c, mix 650 ms, e, mix 500 ms) or presence (b, mix 300 ms; d, mix 300 ms; f, mix 500 ms) of Aβ1–40. Peptide : drug at a 1 : 2 molar ratio. Samples were dissolved in PBS, pH 7.4 (**A** and **B**), or pH 12 (**C** and **D**) at 5 °C, or in DMSO (**E** and **F**) at 37 °C.

reported in ESI†, S6). In our experimental conditions, the co-incubation with tetracycline did not modify the secondary structure of the peptides. In fact, both peptides in PBS, pH 7.4, showed the infrared response characteristic of oligomers. In contrast, Aβ1–40 in PBS at pH 12, as well as in DMSO, was found to be in unordered monomeric form (Fig. 3).

Considering that tetracycline is known to prevent the aggregation of a variety of amyloidogenic proteins and peptides, the finding that the drug does not bind a specific Aβ peptide epitope raises the question of the drug mechanism of action at molecular level. We therefore analyzed tetracycline-Aβ peptide interactions by DLS and AFM.

DLS and AFM analysis of supramolecular complexes

These two techniques were employed aiming the structural characterization of the complexes at the supramolecular level. They are complementary for what concerns the accessible timescales of the aggregation process. In particular, DLS has been shown to be sensitive to the first stages of complex formation. Samples of Aβ1–40 alone, or mixed with tetracycline at a 1 : 8 molar ratio, were analyzed immediately after preparation to observe the initial assembly of the peptide and to minimize the presence of pre-formed seeds. The weight-average hydrodynamic diameter D_H of the particles present into the two samples is reported in Fig. 6a. As previously described,[26] the size of the oligomeric assemblies of Aβ1–40, dissolved in PBS, pH 7.4, increases slowly with time, reaching a value D_{Hfin} after 24 h, (open symbols in Fig. 6a). The analysis of this early-stage kinetics fits with a growth curve described by the equation $D_H(t) = D_{Hfin}\,[1-\exp(-t/\tau)]$ that has a characteristic time $\tau = 4$ h, indicative of a nearly seeds-free sample. The addition of tetracycline to freshly dissolved Aβ1–40 immediately triggered the formation of much larger aggregates (full symbols in Fig. 6a). Noteworthly, such larger aggregates are very stable and do not show any later-stage evolution. Light scattering measurements performed at longer intervals of time (48 h) showed that the Aβ1–40 sample underwent an extensive aggregation process, at variance with the sample

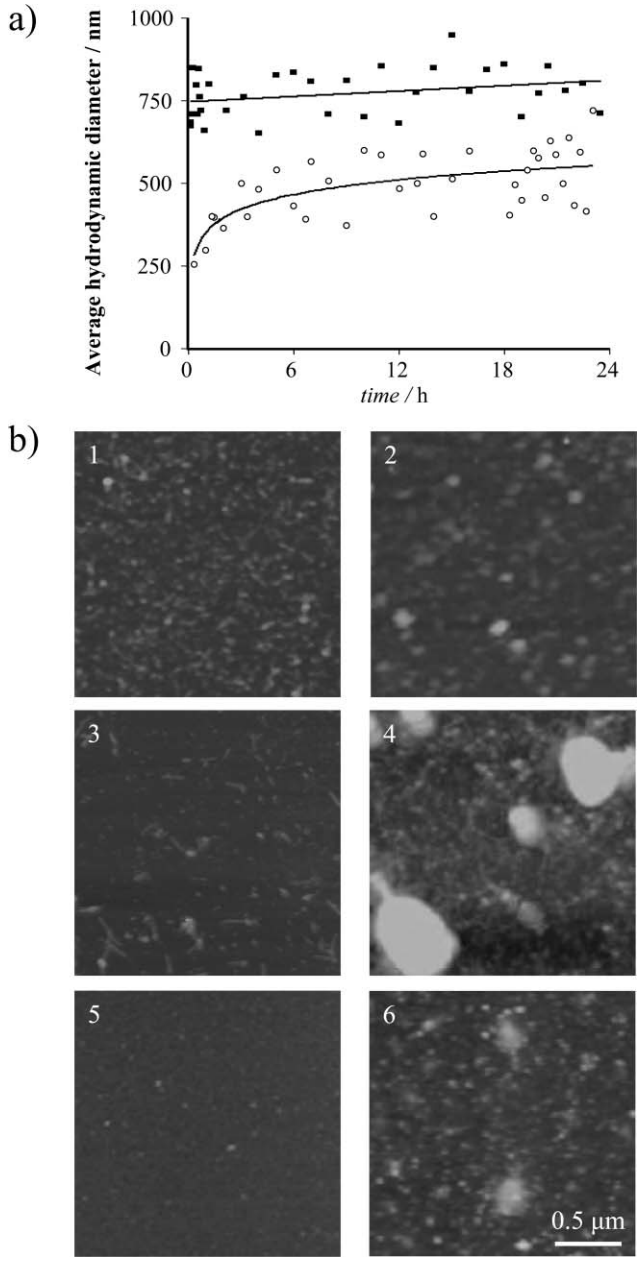

Fig. 6 a) Short-time-evolution of the weight-average hydrodynamic diameter of Aβ1–40 aggregates in aqueous solution determined by dynamic laser light scattering in the presence (full symbols) or in the absence (open symbols) of tetracycline at peptide : drug 1 : 8 molar ratio. b) Atomic force microscopy images of freshly dissolved Aβ1–42 in the absence (1) or presence of tetracycline (2) at a 1 : 4 molar ratio; and after 120 h of incubation at 5 °C in the absence (3) or presence of tetracycline (4); Aβ1–40 after 120 h of incubation in the absence (5) or presence of tetracycline (6).

co-incubated with tetracycline that maintained the same state of aggregation.

AFM studies were carried out to clarify the nature of the assemblies formed by co-incubation of Aβ peptides and tetracycline. Immediately after co-dissolution of Aβ1–42 and tetracycline, clustered material was visible in the form of dispersed aggregates with bigger weight than the regularly distributed background of oligomers (peptide alone, mean and confidence interval, 1.56 nm, 1.23–1.90 nm *vs.* peptide-tetracycline 2.94 nm, 2.54–3.34 nm, $p < 0.0001$ according to t-test). After 120 h, bigger shaped clusters were observed (peptide alone 3.42 nm, 2.76–4.09 nm *vs.* peptide-tetracycline 16.96 nm, 13.99–19.92 nm, $p < 0.0001$). The same trend, although at lesser extent, was observed for Aβ1–40 after 120 h of incubation (peptide alone 0.38 nm, 0.33–0.44 nm *vs.* peptide-tetracycline 1.66 nm, 1.38–1.95 nm, $p < 0.0001$) (Fig. 6b; ESI†, S7).

Tetracycline competes with thioflavin T for binding to Aβ

Tetracycline competes with Thioflavin T (ThT) for binding to Aβ peptides. ThT (Scheme 2) is a benzothiazole dye that exhibits enhanced fluorescence upon binding to amyloid fibrils *ex vivo* and *in vitro*.[27] Recently, it has been found that ThT can also bind Aβ oligomers.[28]

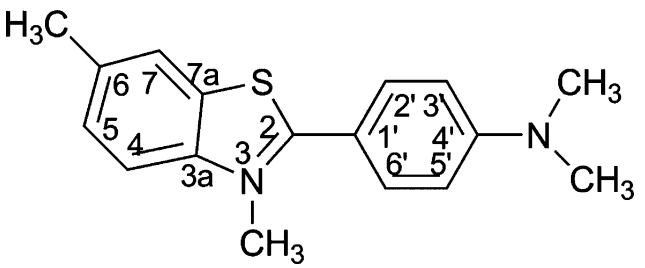

Scheme 2 Thioflavin T structure; numbering of hydrogens and carbons.

This molecule is usually employed to monitor the aggregation process of Aβ peptides and quantify the formation of amyloid fibrils in the absence or presence of anti-amyloidogenic compounds. In experiments aimed at evaluating tetracycline efficacy in hindering Aβ fibrillogenesis, we observed that the drug competes with ThT in binding to peptides.

Under our experimental conditions, tetracycline interfered with ThT fluorescence suggesting the presence of a direct interaction or a competitive binding to Aβ oligomers, as it was recently reported by Hudson *et al.* for polyphenols.[29] To clarify this point, we performed competitive binding experiments by NMR. Firstly, we determined the feasibility of STD-NMR studies to detect ThT binding to Aβ1–40 and Aβ1–42 oligomers, which was proven to be successful. Then, competitive titration STD experiments were performed. In particular, different concentrations of tetracycline were mixed with a solution containing Aβ1–40 or Aβ1–42 (80 uM, PBS, pH 7.4, 25 °C) and ThT, to obtain ThT : tetracycline molar ratios of 1 : 0, 1 : 0.25, 1 : 0.5 and 1 : 1. For each molar ratio, a STD spectrum was acquired and the fractional STD effect on the ThT protons was determined. The alternative protocol was also performed, by mixing solutions of Aβ peptides and tetracycline with different concentrations of ThT. It was observed that, in both cases, the addition of the second ligand to the mixture reduced the STD effect of the first ligand pre-incubated with peptides. The residual fractional STD effect of ThT was higher than that of tetracycline, as an indication of its higher affinity for oligomers (Table 3).

The better interaction for ThT results were also confirmed by tr-NOESY experiments acquired on Aβ1–40 or Aβ1–42 : ThT : tetracycline mixture (ESI†, S8). Indeed, the tr-NOESY spectra showed all tetracycline cross peaks with negative sign only when the tetracycline : ThT molar ratio was 1 : 0.5. For higher

Table 3 Decrease of the fractional STD effect of H8 tetracycline and H7 ThT protons as a function of different compound molar ratios

Tetracycline : ThT ratio	Tetracycline H8 fractional STD effects[a]	ThT H7 fractional STD effects[a]
0 : 1	—	1.00
0.25 : 1	—	0.95
0.5 : 1	—	0.92
1 : 1	0.18	0.82
1 : 0.5	0.64	—
1 : 0.25	0.76	—
1 : 0	1.00	—

[a] Fractional STD effects were calculated as $(I_0–I)/I_0$, where $(I_0–I)$ is the peak intensity in the STD spectrum and I_0 is the peak intensity in the off-resonance spectrum. The largest STD effect ($I_{0\,STD}$) was set to 1 and relative intensities (I_{STD}) were determined.

molar ratios of ThT the tetracycline cross peaks turned to be positive indicating that ThT was able to displace the interaction of the antibiotic with the oligomers. This competitive features were not due to a major change in the structure of the oligomers, since FTIR experiments permitted to verify that the major structural features of the two peptides were non altered by the presence of ThT (ESI†, S9).

The ability of tetracycline to prevent ThT binding to Aβ1–40 and Aβ1–42 oligomers, even if at higher concentrations, further supports tetracycline capability to bind Aβ peptides.

Experimental

Peptide synthesis and purification

Aβ1–40, and Aβ1–42 were prepared by solid-phase peptide synthesis on a 433A synthesizer (Applied Biosystems) using Fmoc-protected L-amino acid derivatives, NOVASYN-TGA resin on a 0.1 mM scale.[26] Peptides were cleaved from the resin as previously described and purified by reverse phase HPLC on a semi-preparative C4 column (Waters) using water–acetonitrile gradient elution.[30] Peptide identity was confirmed by MALDI-TOF analysis (model Reflex III, Bruker). Peptide purity was always above 95%.

Preparation of peptide batch solutions

Aβ1–40 was treated as previously described[31] to obtain reproducible, disaggregated preparations containing only monomers and small oligomers. For Aβ1–42 experiments a batch was selected that contained pre-amyloidogenic seeds highly toxic to N2a cells. Immediately before use, lyophilized Aβ1–40 and Aβ1–42 were dissolved in 10 mM NaOH in 9 : 1 H_2O : D_2O or D_2O at variable concentrations, then diluted 1 : 1 with 10 mM phosphate buffer saline, pH 7.4 containing 150 mM NaCl (PBS). The pH of each sample was verified with a Microelectrode (Mettler Toledo) for 5 mm NMR tubes and adjusted with NaOD or DCl. For samples dissolved in D_2O, all pH values were corrected for isotope effects. To avoid bacterial contamination NaN_3 0.01% w/v was added to samples in 9 : 1 H_2O : D_2O. In the experiments carried out up to 120 h, samples were kept at 5 °C to minimize Aβ peptide aggregation and tetracycline oxidation and precipitation.

In vitro toxicity assay

Aβ1–42 was dissolved in 10 mM NaOH and mixed with tetracycline solution in PBS to obtain peptide : drug molar ratios of 1 : 4 or 1 : 8. Solutions were then incubated under static conditions at 37 °C for 70 h. Aliquots of peptide were also incubated in PBS in the absence of tetracycline. Peptide solutions were serially diluted in Dulbecco's MEM (DMEM) immediately before cell treatment. N2a cells were harvested in DMEM supplemented with 10% fetal calf serum (FCS). For toxicity assays, cells were trypsinized and 100 µl of 5×10^4 cell/ml suspension in DMEM with 1% FCS were plated (96 multiwell plates, Iwaki). Four h after plating, 10 µl aliquots of different Aβ1–42 solutions were added to the cell medium; cell impairment was evaluated after 24 h incubation using the MTT reduction assay (Sigma-Aldrich).

SDS-PAGE and DOT BLOT assay

Peptide solutions were diluted 1 : 1 with loading buffer containing 12% (w/v) SDS (sodium dodecyl sulfate) and 100 mM dithiothreitol in 0.5 M Tris-HCl buffer, pH 6.8, and immediately denatured at 100 °C for 5 min. Samples were analyzed by electrophoresis on 1.5 mm thick 12.5% polyacrylamide gels (SDS-PAGE) followed by Western Blot analysis with anti-Aβ primary antibody 6E10 (Signet Laboratories) and anti-mouse peroxidase-conjugated secondary antibody (DAKO). Antibody binding was detected by chemoluminescence (ECL detection system, GE Healthcare). For Dot Blot assays, 4 µg aliquots of Aβ1–42 were spotted on nitrocellulose membranes (0.2 µm filter paper, Whatman); after air drying the membranes were blocked overnight in 10 mM Tris-HCl, pH 7.4, 100 mM NaCl, 0.1% Tween-20 (TBST) supplemented with 5% non-fat milk. Membranes were washed in TBST and incubated sequentially with A11 anti-oligomer antibody[32] (Biosource) and anti-rabbit peroxidase-conjugated secondary antibody (Sigma). Antibody binding was detected by chemoluminescence.

NMR spectroscopy

NMR experiments were recorded on a Varian 400-MHz Mercury or a Bruker 600-MHz Advance equipped with a Bruker CryoProbe. Both spectrometers were equipped with a *z*-axis gradient coil. Tetracycline was dissolved in PBS, pH 7.4 or 12, or in d_6-DMSO (methyl sulfoxide), and then added to the peptide solution. Basic sequences were employed for 2D-TOCSY, 2D-NOESY, diffusion and STD experiments. ^{1}H spectra were acquired with 128, 160, 256 or 512 transients and 2 s recycle delay. 2D-TOCSY spectra were recorded with 16 or 32 transients, 256 t_1 increments, 1 s recycle delay, a mixing time between 60 and 120 ms, and with a spin-lock pulse of nearly 7000 Hz. 2D-NOESY spectra were recorded with 64, 72, 80 or 96 transients and 256 t_1 increments, a recycle delay variable between 1 and 2.5 s, and a mixing time between 100 and 800 ms. The spectral width was varied between 4504 and 6006 Hz. Peptide spin systems were initially identified using the 2D-TOCSY spectra. Intra-residue and sequential inter-residue connectivities were then assigned using the 2D-NOESY spectra. For STD, a train of Gaussian-shaped pulses each of 50 ms was employed to saturate selectively the protein envelope; the total saturation time of the protein envelope was varied between 5 s and 0.5 s. For experiments in H_2O solvent, the WATERGATE or the excitation sculpting solvent suppression was employed.

Diffusion experiments were performed employing an array of 20 or 30 spectra for each experiment (128, 256 or 512 transients each, with a 1 or 2 s recycle delay) varying the gradient strength from 3.33 to 19.4 G/cm^2. The lengths of and delays between the gradient pulses were optimized depending on the experimental conditions and ranged between 0.002 and 0.005 s and 0.2–0.7 s, respectively. Data fitting and diffusion coefficients determination were performed with the software *Dosytoolbox*.[33]

Dynamic laser light scattering (DLS)

DLS measurements were performed on a custom apparatus[34] using a diode laser (λ = 532 nm) and a digital correlator (Brookhaven Instruments Co). Samples (c = 0.65 mg ml^{-1}) were kept at controlled temperature (T = 37 °C). The scattered intensity correlation functions were analysed with the cumulant analysis method[35] giving the weight average hydrodynamic diameter of the particles in solution.

Atomic force microscopy (AFM)

For AFM analysis peptide samples were diluted to 5 μM with 10 mM HCl and 60 μl aliquots were immediately spotted onto a freshly cleaved Muscovite mica disk and incubated for 0.5 min. The disk was then washed with H_2O and dried under a gentle nitrogen stream. Samples were mounted onto a Multimode AFM with a NanoScope V system (Veeco/Digital Instruments) operating in Tapping Mode using standard phosphorus-doped silicon probes (T: 3.5–4.5 μm, L: 115–135 μm, W: 30–40 μm, f_0: 311–364 kHz, K: 20–80 N m^{-1}) (Veeco).

FTIR spectroscopy

FTIR spectra were measured in transmission on the same samples examined by NMR spectroscopy. Twenty μl of the peptide D_2O solutions were placed between 2 BaF_2 windows separated by a 100 μm Teflon spacer. FTIR spectra were recorded using a FTS40A spectrometer (Bio-Rad, Digilab Division, Cambridge, MA) equipped with a nitrogen-cooled mercury–cadmium–tellurium (MCT) detector under the following conditions: 2 cm^{-1} spectral resolution, 1000 scan co-addition, 25 kHz scan speed, and triangular apodization. Peptide spectra were obtained after subtraction of the buffer spectrum from that of the peptide solution. Second-derivatives of the absorption spectra[36] were performed to resolve the secondary structure and aggregate components that overlap into the broad and structureless Amide I band in the measured spectrum. This mathematical procedure permitted the identification of the different components that give rise to negative bands in the derivative spectrum, and whose minima correspond to the component peaks in the measured spectrum. For this analysis the Savitsky–Golay (5 points) procedure was employed after binomial smoothing of the absorption spectra (11 points).

Circular Dichroism (CD)

Spectra were recorded by the JASCO J-815 spectropolarimeter (JASCO corporation, Tokyo, Japan) under the following conditions: scanning speed 10 nm min^{-1}, band width 1 nm, 5 accumulations per sample, and 0.1 cm path length cuvette.

Theoretical basis of PFG-NMR diffusion measurements

Pulse field gradient (PFG) NMR diffusion measurements allow molecular size estimation through the measurement of diffusion coefficients.[37] The diffusion coefficient is inversely proportional to the hydrodynamic radius of the particle as described by the Stokes–Einstein equation:

$$D_T = \frac{k_B T}{6\pi\eta R'}$$

where D is the diffusion constant, k_B is the Boltzmann constant, T is temperature, η is viscosity and R' the hydrodynamic radius. The hydrodynamic radius is scaled with a power law of the mass.

Differences in peptide aggregation state, or the addition of peptide or tetracycline to the sample, affected the viscosity of the solution and thereby the measured diffusion coefficient. This was accounted for by measuring the HDO diffusion and then correcting the measured values according to the following equation:[38]

$$D_{corrected} = \frac{D_{HDO,neat}}{D_{HDO,measured}} D_{observed}$$

In our case, HDO_{neat} values for PBS buffer used for peptide dissolution were determined at 5, 25 and 37 °C.

When two substances, a ligand and a receptor, interact, there is a change both in their mass and in most cases, shape. When the ligand is in fast exchange between the bound and the free states on the timescale of the diffusion experiment, the measured diffusion coefficient is the weighted mean value of the free and bound states.

$$D_{observed} = (1 - p_{complex})D_{free} + p_{complex}D_{complex}$$

When the equilibrium between the ligand free state and the ligand bound state is fast on the translational diffusion time scale (ms), it leads to an averaged observed diffusion coefficient, higher than that expected for the complex, but lower than that expected for the free ligand. This makes the diffusion coefficient a sensitive observable parameter when measuring ligand-receptor interactions.

Conclusions

The present study was prompted by the observation that tetracycline can reduce the *in vitro* toxicity of oligomeric Aβ1–42 in a dose-dependent manner. This is a particularly important finding since oligomers are considered the neurotoxic species which play a pivotal role on the onset and progression of AD. NMR and FTIR studies have unveiled the capacity of tetracycline to interact with Aβ peptides in a non-conventional manner, as shown by the absence of a specific epitope in the drug and the absence of a well-defined binding site on the Aβ peptides. Noteworthy, NMR data showed for the first time that tetracycline competes with ThT in the binding to Aβ peptides.

DLS and AFM also indicated that supramolecular complexes are immediately formed when Aβ peptides are co-dissolved with tetracycline, preventing the formation of aggregates. Incubation of both Aβ peptides with tetracycline led to the formation of colloidal particles that specifically sequester oligomers, preventing in this way the progression of the amyloid cascade. We can hypothesize that the internal structure of aggregates formed by Aβ

peptides with tetracycline is disordered and non-homogeneous, governed by hydrophobic and charge multiparticle interactions. The formation of supramolecular aggregates that improve the solubility of Aβ peptides is in good agreement with a recent report on the mechanism of action of small anti-amyloidogenic molecules.[39] However, in contrast to the molecules studied by those authors, tetracycline does not spontaneously form colloidal aggregates in aqueous solution.

Our observations shed light on the anti-fibrillogenic activity of tetracycline with both Aβ and other amyloidogenic proteins. These data may be useful for the development of novel tetracycline analogues devoid of antibiotic activity for the treatment of brain and peripheral amyloidosis. In addition, the experimental protocol here described can be applied to the screening of new potential Aβ ligands showing anti-amyloidogenic properties and to the characterization of their mechanism of action at molecular level.

Acknowledgements

The research leading to these results has received funding from the European Community's Seventh Framework Programme (FP7/2007-2013) under grant agreement n 212043. We acknowledge the Italian Ministry of Health (533F/Q/1), Cariplo Foundation (Project NOBEL-GUARD), Banca IntesaSanPaolo, and PRIN (PROT.2007T7MSAJ) for financial support and Flamma (Italy) for the kind gift of Fmoc amino acids.

Notes and references

1 J. Hardy and D. Allsop, *Trends Pharmacol. Sci.*, 1991, **12**, 383–388.
2 C. J. Pike, D. Burdick, A. J. Walencewicz, C. G. Glabe and C. W. Cotman, *J Neurosi*, 1993, **13**, 1676–1687.
3 D. J. Selkoe, *Ann. N. Y. Acad. Sci.*, 2000, **924**, 17–25.
4 K. Ono and M. Yamada, *J. Neurochem.*, 2006, **97**, 105–115.
5 I. Cardoso, G. Merlini and M. J. Saraiva, *FASEB J.*, 2003, **17**, 803–809.
6 G. Forloni, M. Salmona, G. Marcon and F. Tagliavini, *Infectious disorders: drug targets*, 2009, **9**, 23–30.
7 E. Ilyina, V. Roongta, H. Pan, C. Woodward and K. H. Mayo, *Biochemistry*, 1997, **36**, 3383–3388.
8 J. Danielsson, J. Jarvet, P. Damberg and A. Graslund, *Magn. Reson. Chem.*, 2002, **40**, S89–S97.
9 W. B. Stine Jr., K. N. Dahlgren, G. A. Krafft and M. J. LaDu, *J. Biol. Chem.*, 2003, **278**, 11612–11622.
10 P. Groves, M. O. Rasmussen, M. D. Molero, E. Samain, F. J. Canada, H. Driguez and J. Jimenez-Barbero, *Glycobiology*, 2004, **14**, 451–456.
11 Insulin is a dimer at 37 °C; M. Lin and C. K. Larive, *Anal. Biochem.*, 1995, **229**, 214–220.
12 G. Habicht, C. Haupt, R. P. Friedrich, P. Horstchansky, C. Sachse, J. Meinhardt, K. Wieligmann, G. P. Gellerman, M. Brodhun, J. Gotz, K. J. Halbhuber, C. Rocken, U. Horn and M. Fandrich, *Proc. Natl. Acad. Sci. U. S. A.*, 2007, **104**, 19232–19237.
13 E. Cerf, R. Sarroukh, S. Tamamizu-Kato, L. Breydo, S. Derclaye, Y. Dufrêne, V. Narayanaswami, E. Goormaghtigh, J. M. Ruysschaert and V. Raussens, *Biochem. J.*, 2009, **421**, 415–523.
14 J. L. Arrondo, F. J. Blanco, L. Serrano and F. M. Goni, *FEBS Lett.*, 1996, **384**, 35–37.
15 A. Natalello, V. V. Prokorov, F. Tagliavini, M. Morbin, G. Forloni, M. Beeg, C. Manzoni, L. Colombo, M. Gobbi, M. Salmona and S. M. Doglia, *J. Mol. Biol.*, 2008, **381**, 1349–1361.
16 J. L. Arrondo and F. M. Goñi, *Prog. Biophys. Mol. Biol.*, 1999, **72**, 367–405.
17 M. Jackson and H. H. Mantsch, *Biochim. Biophys. Acta.*, 1991, **1078**, 231–235.
18 B. Meyer and T. Peters, *Angew. Chem., Int. Ed.*, 2003, **42**, 864.
19 M. Mayer and T. L. James, *J. Am. Chem. Soc.*, 2002, **124**, 13376–13377.
20 S. Di Micco, C. Bassarello, G. Bifulco, R. Riccio and L. Gomez-Paloma, *Angew. Chem., Int. Ed.*, 2006, **45**, 224–228.
21 F. Souard, E. Munoz, P. Penalver, C. Badia, R. Del Villar-Guerra, J-Luis Asensio, J. Jimenez-Barbero and C. Vicent, *Chem.–Eur. J.*, 2008, **14**, 2435–2442.
22 L. Mengfen, M. J. Shapiro and J. R. Wareing, *J. Am. Chem. Soc.*, 1997, **119**, 5249–5250.
23 L. H. Lucas and C. K. Larive, *Concepts Magn. Reson.*, 2004, **20A**, 24–41.
24 We tried the deconvolution of DOSY spectra. We used the DOSYtoolbox by M. Nillson, and G. Morris. Results of our analysis are reported in ESI S3†.
25 D. Neuhaus, M. P. Williamson, *The kinetics of the NOE in The Nuclear Overhauser Effect in Structural and Conformational Analysis*, VCH Publishers Inc., New York, 1986, pp. 103–140.
26 G. Di Fede, M. Catania, M. Morbin, G. Rossi, S. Suardi, G. Mazzoleni, M. Merlin, A. R. Giovagnoli, S. Prioni, A. Erbetta, C. Falcone, M. Gobbi, L. Colombo, A. Bastone, M. Beeg, C. Manzoni, B. Francescucci, A. Spagnoli, L. Cantù, E. Del Favero, E. Levy, M. Salmona and F. Tagliavini, *Science*, 2009, **323**, 1473–1477.
27 R. Khurana, C. Coleman, C. Ionescu-Zanetti, S. A. Carter, V. Krishna, R. K. Graver, R. Roy and S. Singh, *J. Struct. Biol.*, 2005, **151**, 229–238.
28 I. Maezawa, H. S. Hong, R. Liu, C. Y. Wu, R. H. Cheng, M. P. Kung, H. F. Kung, K. S. Lam, S. Oddo and F. M. La Ferla, *L. W. J. Neurochem.*, 2008, **104**, 457–468.
29 S. A. Hudson, H. Ecroyd, T. W. Kee and J. A. Carver, *FEBS J.*, 2009, **276**, 5960–5972.
30 M. Salmona, M. Morbin, T. Massignan, L. Colombo, G. Mazzoleni, R. Capobianco, L. Diomede, F. Thaler, L. Mollica, G. Musco, J. J. Kourie, O. Bugiani, D. Sharma, H. Inouye, D. A. Kirschner, G. Forloni and F. Tagliavini, *J. Biol. Chem.*, 2003, **278**, 48146–4815.
31 C. Manzoni, L. Colombo, M. Messa, A. Cagnotto, L. Cantù and E. Del Favero, *Amyloid*, 2009, **16**, 71–80.
32 R. Kayed, E. Head, J. L. Thompson, T. M. McIntire, S. C. Milton, C. W. Cotman and C. G. Glabe, *Science*, 2003, **300**, 486–489.
33 http: // personalpages . manchester . ac . uk / staff / mathias . nilsson / software.htm.
34 P. Lago, L. Rovati, L. Cantù and M. Corti, *Rev. Sci. Instrum.*, 1993, **64**, 1797–1802.
35 D. E. Koppel, *J. Chem. Phys.*, 1972, **57**, 4814–4820.
36 H. Susi and D. M. Byler, *Methods Enzymol.*, 1986, **130**, 290–311.
37 P. Stilbs, *Anal. Chem.*, 1981, **53**, 2135–2137.
38 J. Danielsson, J. Jarvet, P. Damberg and A. Graslund, *Biochemistry*, 2004, **43**, 6261–6269.
39 B. Y. Feng, B. H. Toyama, H. Wille, D. W. Colby, S. R. Collins, B. C. H. May, S. B. Prusiner, J. Weissman and B. K. Shoichet, *Nature Chemical Biology*, 2008, **4**, 197–199 .

